IEEE Access
Multidisciplinary | Rapid Review | Open Access Journal

Received 5 October 2023, accepted 30 October 2023, date of publication 8 November 2023, date of current version 14 November 2023.

Digital Object Identifier 10.1109/ACCESS.2023.3331106

RESEARCH ARTICLE

Leaky-Wave Antenna Array With Bilateral Beamforming Radiation Pattern for Highly Efficient Mobile Communication System

YULU ZHANG, JUNHONG WANG, (Senior Member, IEEE), AND YUNJIE GENG, (Member, IEEE)

Key Laboratory of All Optical Network and Advanced Telecommunication Network, Ministry of Education, Institute of Lightwave Technology, Beijing Jiaotong University, Beijing 100044, China

Corresponding author: Junhong Wang (wangjunh@bjtu.edu.cn)

This work was supported in part by the National Natural Science Foundation of China under Grant 62031004 and Grant 62221001.

ABSTRACT In this paper, a leaky-wave antenna (LWA) array based on substrate integrated waveguide (SIW) is proposed for generating bilateral secant-distributed radiation pattern, which can cover a wide angular range including broadside direction. The LWA array contains two antenna elements and a power recycling network. Each element contains a composite slot constructed by superposing three continuous cosine-shaped slots with different periods in a weighted way, which can achieve a unilateral beam-forming radiation pattern. The power recycling network makes the waves in adjacent antenna elements travel in opposite directions, so the two elements can radiate in reverse directions to generate a bilateral beamforming pattern. The proposed bilateral radiation LWA array is fabricated and measured to verify the efficiency of the design, and the measurement results are in good agreement with those of simulations.

INDEX TERMS Bilateral beamforming pattern, leaky-wave antenna (LWA), power recycling network, composite slot.

I. INTRODUCTION

Nowadays, mobile communications are extended to various complex environments to meet different requirements. The quality and reliability of mobile communication are mainly determined by radio wave coverage, which further depend on the antenna performances [1]. The mobile communication performance can be improved by both terminal antennas and base station antennas. Many kinds of terminal antennas have been proposed for 5G smartphone [2], [3], [4], which show excellent impedance matching, port isolation, antenna efficiency and envelope correlation coefficient. For a base station, when using antennas with wide beamwidth to cover flat area or straight path, the field coverage is non-uniform and the effective covering area or distance is small. As a result, the efficiency of the entire mobile communication system is very low. Therefore, antennas with secant radiation patterns, which can achieve flatter radio wave coverage in desired areas or straight paths [5], are employed to replace the wide beamwidth antennas.

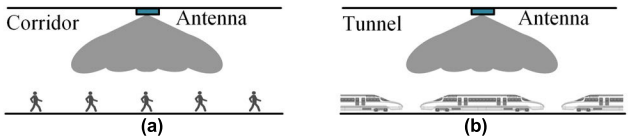

FIGURE 1. Application diagrams of the bilateral beam-formed antenna. (a) In corridor, (b) in tunnel.

Leaky-wave antenna based on SIW exhibits excellent characteristics, such as simple feeding structure, frequency scanning and easy integration. LWAs usually generate radiation through different shaped slots cut in their wall, such as transversal slots [6] or long horizontal slots [7]. It is well known that a desired radiation pattern can be synthesized by adjusting the aperture size and shape of LWA,

The associate editor coordinating the review of this manuscript and approving it for publication was Wanchen Yang.

and many works have been done in this aspect. In [8], LWAs with low SLL are proposed by meandering a long slot on the top wall or meandering the side vias of SIW, whose aperture shapes satisfy Taylor distribution. Recently, a series of LWAs with secant-squared beamforming radiation patterns are proposed by superposing slots with different periods in a weighted way [9], [10], [11], [12]. However, most of the available beam-forming LWAs are designed for unilateral secant beamforming patterns, and the angular ranges of beamforming are a litter bit narrow. In addition, open stopband (OSB) usually appears in periodic LWA structure when the radiation beam points to broadside [13]. Thus, the beamforming ranges of many beamforming LWAs don't cover the broadside direction. Techniques concerned with OSB removing are proposed by introducing extra slots near the radiation slots to cancel the reflection, but making the structures more complex and fabrication more difficulty. Furthermore, antennas with bilateral beamforming radiation patterns are usually required in some application scenarios. As shown in Fig. 1, using bilateral beam-forming antenna as the base station antenna, trains in the tunnel or users in the long straight corridor can receive stable radio wave when approaching or moving away from the antenna.

In this work, a composite slot LWA array with power-recycling network [14] is proposed for bilateral beamforming radiation including broadside direction. As the composite slot structure exhibits non-periodic property, OSB is naturally removed. In addition, the power-recycling network can reuse the non-radiated energy, which makes the waves in adjacent waveguides travel in opposite directions to generate opposite radiation. Therefore, bilateral beam-forming pattern including broadside is achieved.

II. THEORY AND METHOD

For an LWA designed on SIW, the analysis of it can be equivalent to that of a traditional LWA designed on dielectric-filled rectangular waveguide with dielectric constant ε_r and equivalent width of [14]

$$w_{eff} = a - 1.08 \times \frac{d^2}{s} + 0.1 \times \frac{d^2}{a}, \tag{1}$$

where a is the width of SIW, d and s are the diameter of the metal vias and the distance between adjacent vias, respectively. According to the radiation mechanism of periodic leaky wave structure, spatial harmonics will be generated by LWA, and the beam direction of the mth spatial harmonic is [15]

$$\theta_m = \sin^{-1}[\sqrt{\varepsilon_r - (\lambda_0/2w_{eff})} + m\lambda_0/p], \tag{2}$$

where λ_0 is the free space wavelength, and p is the period of slots.

Three continuous cosine-shaped slots with periods p_n [9] are used as the basic radiation structures, as shown in Fig. 2,

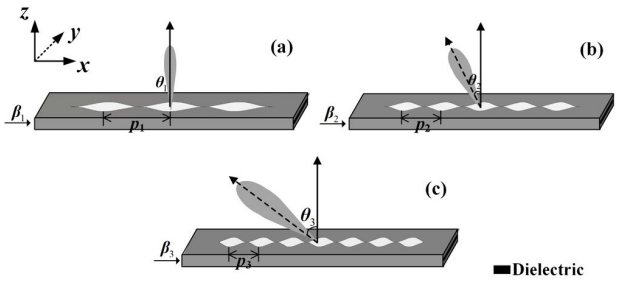

FIGURE 2. LWAs with different continuous cosine-shaped slots. (a) LWA with period p_1. (b) LWA with period p_2. (c) LWA with period p_3.

which are expressed by

$$x = w_n \times \cos(\frac{2\pi}{p_n} \times y) + w_n, -ls/2 \le y \le ls/2, n = 1, 2, 3 \tag{3}$$

where w_n is the weighting coefficient of each cosine slot. ls is the length of the radiation slot.

When the three slots are superposed in a weighted way, a composite slot which can generate unilateral cosecant-distributed beamforming pattern including broadside direction is obtained, as shown in Fig. 3(a). The structure parameter of the composite slot is given by

$$x = \sum_{n=1}^{3} [w_n \times \cos(\frac{2\pi}{p_n} \times y) + w_n], -ls/2 \le y \le ls/2, \quad n = 1, 2, 3, \tag{4}$$

To get a bilateral secant-distributed radiation pattern covering broadside radiation, two composite slots are arranged into an LWA array, and a power-recycling network for forward and backward beam-forming radiation is used, as shown in Fig. 3(b).

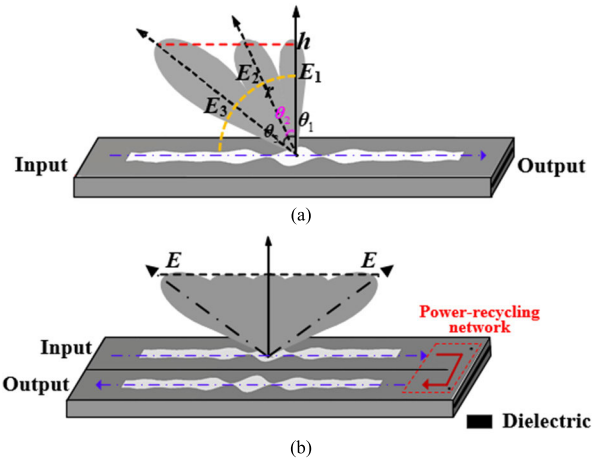

FIGURE 3. Design process of the LWA array with bilateral beam-forming radiation pattern. (a) Unilateral beam-forming LWA with composite slot. (b) Bilateral beam-forming LWA array with power recycling network.

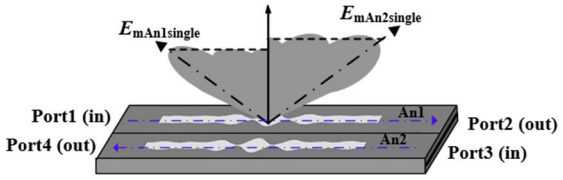

FIGURE 4. Radiation patterns of the array elements when fed individually.

Fig. 3(a) also shows the relationship between the radiation strength and the beam angles of the secant-distributed radiation pattern. To get the same E-field amplitude along a horizontal line with a distance h from the antenna, radiation fields E_n of the three beams should satisfy the following relationships [8]:

$$E_1 : E_2 : E_3 = \sec\theta_1 : \sec\theta_2 : \sec\theta_3. \tag{5}$$

Particularly, for an LWA array with power-recycling network shown in Fig. 3(b), part of the input energy has already been radiated by An1, so the input power of An2 is less than that of An1. If the two array elements have the same slot size, the array will generate an unbalanced bilateral radiation pattern. Therefore, the slot in An2 should be designed with a larger size (increasing the radiation strength) to compensate for the attenuation of the power due to radiation of An1. If denoting the maximum radiation E-field amplitudes using $E_{\mathrm{mAn1single}}$ and $E_{\mathrm{mAn2single}}$ for An1 and An2 excited by the same input power separately, as shown in Fig. 4, then $E_{\mathrm{mAn1single}}$ and $E_{\mathrm{mAn2single}}$ should satisfy:

$$E_{\mathrm{mAn1single}} = |S_{21}| \cdot E_{\mathrm{mAn2single}}. \tag{6}$$

where S_{21} is the S-parameter of An1.

III. ANTENNA DESIGN

The proposed SIW LWAs are designed on a 3 mm thick F4BM substrate with permittivity of $\varepsilon_r = 3$ and loss tangent of 0.0015. The working frequency is 5.8 GHz.

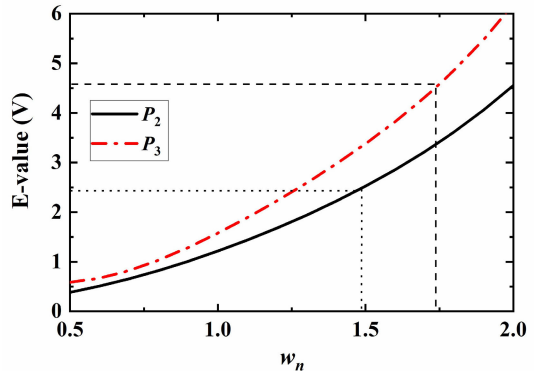

FIGURE 5. Relationships between E-field strength and weighting coefficients of the cosine-shaped slots with periods p_2, p_3.

Based on the theory mentioned above, the unilateral beam-formed pattern is composed of three beams pointing to 0°, −20° and −60°, and the corresponding slot periods are p_1, p_2 and p_3, respectively. The first step is to superpose two slot structures with radiation beams at −20° and −60° in a weighted way. According to equation (2), the initial values of p_2, p_3 are set to 30 mm, 23 mm, and the E-field value of corresponding beams should meet formula (5). Thus, two cosine slots with different periods p_2, p_3 are simulated to find the relationships between E_n and coefficient w_n, as shown in Fig. 5. If we choose a value of E_2 on the black solid curve in Fig. 5 (corresponding to w_2 on the horizontal axis), then the value of E_3 can be calculated using formula (5), and the corresponding w_3 can be found from the red dot-dashed curve in Fig. 5. Formula (5) only gives the ratios, and how to determine the initial value of E_2 (corresponding to initial w_{n}) from Fig. 5 is a trade-off between radiation efficiency and input impedance matching. For an LWA, larger size of radiation slot (corresponding to a larger w_{n}) will generate stronger radiation electric field, but usually resulting in worse impedance matching. Based on a lot of testing computations, w_2 and w_3 are chosen as 1.45 and 1.7, respectively, making the beams meet the secant distribution requirement, as shown in Fig. 6(a). The structural parameters need to be further optimized after the cosine-shaped slots with two different periods are superposed into one composite slot for secant pattern. The final optimized values for p_2, p_3, w_2 and w_3 are 31.2 mm, 24.2 mm, 1.4 and 1.47, respectively. The red curve shown in Fig. 6(a) is the radiation pattern of the composite slot antenna, which shows a beam-forming range from −60° to −20°.

The second step is to superpose the cosine-shaped slot corresponding to the broadside direction into the above composite slot using equation (4), and the weight coefficient w_1 is optimized by full-wave simulation for the objective of making the radiation strength meet the secant-distributed relationship. As we know, open stopband (OSB) usually appears in periodic structure when radiating in broadside direction. OSB is caused by the in-phase superposition of reflections from periodic slots at the input port, which results in large reflection and the power cannot be fed into the radiating structure. In this paper, the periodic cosine-shaped slot for broadside radiation is not designed to radiate individually. It is superposed with other periodic cosine slots to construct a composite slot, which is not an exact periodic structure, as shown in Fig. 3(a). The non-periodic property of the composite slot plays a role as those extra non-radiating slots commonly introduced into LWA for OSB suppression, which can cancel the reflection from the periodic radiating slots. Thus, the power at input port can be fed into the composite slot, and a beam-forming pattern with broadside can be obtained.

Similarly, An2 can be designed using the same procedure, whose max E-field amplitude should satisfy formula (6), considering the energy attenuation. The E-filed patterns of the two antennas fed individually are given in Fig. 6(b). These two patterns superposed together

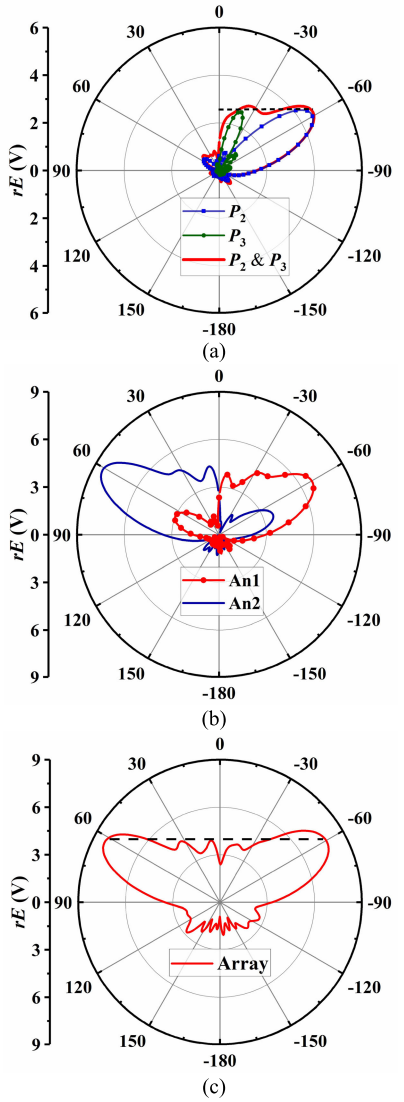

FIGURE 6. Simulated E-patterns of the proposed antennas. (a) E-field patterns of cosine-shaped slots with period of p_2, p_3 and composite slot composed of the two cosine-shaped slots. (b) E-filed patterns of An1 and An2 fed individually. (c) E-field of the proposed array with power recycling network.

TABLE 1. Parameters of the composite slots.

	n	1	2	3
An1	p_n (mm)	40	31	24.5
	w_n	0.87	1.47	1.47
An2	p_n (mm)	44	32.5	25.2
	w_n	0.83	1.67	1.67

TABLE 2. Parameters of the antennas. (UNIT: mm).

a	23	dx_1	13	dp_1	13
d	1.5	dy_1	13	dp_2	12
s	2.5	dx_2	12	dp_3	13
L	245	dy_2	10.5	dp_4	12.5
W	68	dy	16	d_1	1.4
w	39	ls	176	L_1	115
L_2	120	L_3	120.5		

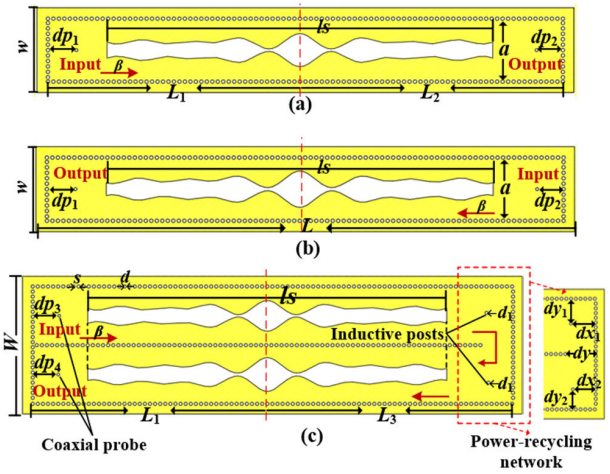

FIGURE 7. Structures of the proposed antennas. (a) Beam-forming antenna for backward radiation (An1). (b) Beam-forming antenna for forward radiation (An2). (c) Bilateral beam-forming antenna array (Array).

can provide a bilateral secant radiation pattern covering broadside direction when the phases of An1 and An2 are designed properly. The superposed secant pattern covering a beam-forming range from −60° to 60° is given in Fig. 6(c).

The proposed antennas are all fed by coaxial probes, and the residual energy at the end of antennas is absorbed by the matching load, as indicated in Fig. 7. The diameter and length of feeding probes are 1.27 mm and 3 mm. As shown in dotted boxes in Fig. 7(c), the locations of the inductive vias in power-recycling feeding network influence the initial phase of the An2, which needs to be optimized. The final parameters of antenna elements are summarized in Table 1. Table 2 gives the detailed parameters of the antennas.

IV. RESULTS AND DISCUSSION

A. SIMULATION AND MEASUREMENT

For validating properties of the proposed antennas, three LWAs (An1, An2, Array) are fabricated, as shown in Fig. 8. The LWAs are measured by Agilent E8363C PNA network analyzer in an anechoic chamber, as shown in Fig. 9. In the radiation performance measurement, the proposed antennas are set to be the receiving antenna, and a standard horn antenna with the same working frequency band is set as the transmitting antenna.

The simulated and measured S-parameters are plotted in Fig. 10 and their radiation properties are given in Table 3. From Fig. 10, it can be seen that the trends of simulated and measured S-parameter curves are basically the same, indicating good impedance matching of the designed antennas, but the resonant point of measured $|S_{11}|$ is offset

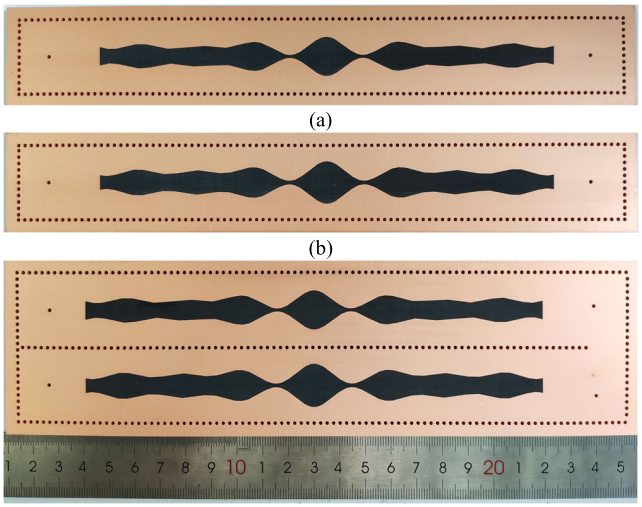

FIGURE 8. Fabricated beam-forming antennas. (a) An1. (b) An2. (c) Array.

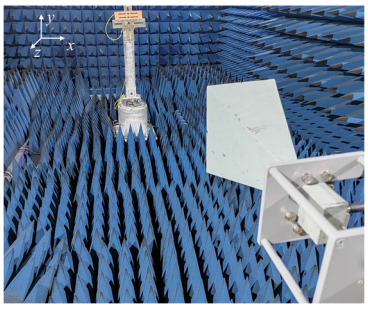

FIGURE 9. Beam-forming antenna in the measured environment.

TABLE 3. Radiation characteristics of the designed SIW LWAs.

	An1	An2	Array
Simlation (dBi) (f = 5.8 GHz)	1.69	3.74	3.63
Measurement (dBi) (f = 5.9 GHz)	2.81	4.31	3.68
Simulated E-value (V/m)	6.65	8.42	8.25
S-parameter (linear)	$\|S_{21}\| = 0.815$		/
Simulated radiation efficiency (%)	20.3%	28.8%	42.8%

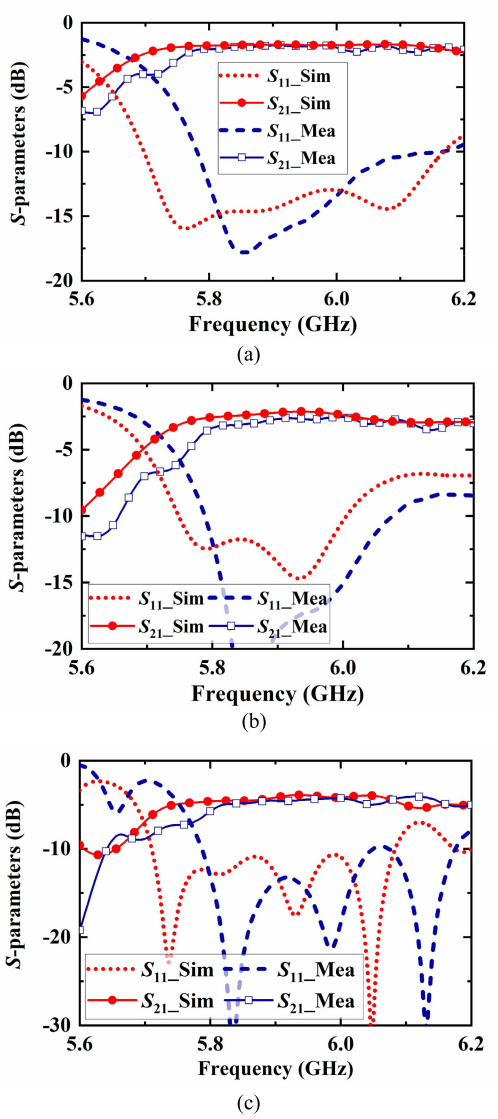

FIGURE 10. Simulated and measured S-parameters of the three SIW LWAs. (a) An1. (b) An2. (c) Array.

from that of simulation about 100 MHz. The differences are mainly caused by the fabrication tolerance and error of the dielectric constant of substrate. Thus, for the radiation property measurement, the operating frequency is selected as 5.9 GHz. In addition, Fig. 10 indicates that the open-stopband is completely removed in the operating frequency band.

Fig. 11 plots the simulated and measured normalized co-polarization and cross-polarization radiation patterns in E-plane of the beam-forming antennas. The measured normalized patterns, main beam angles and the co-polarization in the range of beam-forming are basically in good agreement with simulation results. For the design of beam-forming antennas, whether the beamforming pattern is close to the desired pattern is the main concern of the design. The ideal secant patterns are also given in Fig. 11, showing good agreements between the ideal patterns and the measured results within beamforming range. In addition, the electric length of the proposed antenna is only $3.5\lambda_0$ for getting a wider beam width, so the radiation efficiency of the antenna element is a litter lower. Thus, the power recycling network is used to form an array, which enables the residual power at the end of the first array element An1 to be re-transmitted to the second array element An2 for radiation. This is equivalent to increasing of the length of single antenna to improve the radiation efficiency, as shown in Table 3.

To compare with other beam-forming leaky wave antennas, the characteristic parameters of the proposed antennas are listed in Table 4 together with those of other antennas. Most of the available beamforming LWAs cannot cover the broadside.

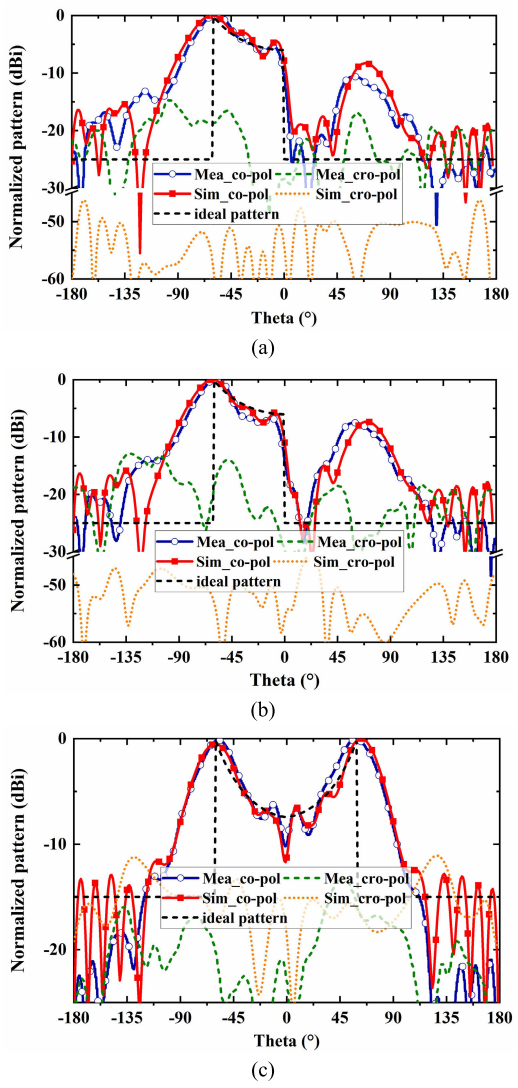

FIGURE 11. Ideal secant pattern, simulated and measured normalized gain patterns of the beam-forming antennas. (a) An1. (b) An2. (c) Array. (The frequency for measurement is 5.9 GHz, and the frequencies for other curves are 5.8 GHz).

Some other types of beamforming antennas can cover the broadside, but the angular range of beamforming is relatively smaller. It can be seen that the proposed leaky-wave antenna array with bilateral radiation pattern can cover a much larger beam-forming range, and exhibits the capability of broadside radiation.

B. ANALYSIS OF POLARIZATION PROPERTIES

To discuss the polarization properties of the designed antennas, the electric field in the radiation aperture is extracted, as shown in Fig. 12. The electric field is perpendicular to the slot edges, which can be decomposed into horizontal and vertical components. The radiation from the vertical components cancels each other, while the radiation from the horizontal components superposes. Thus, horizontal polarization is the main polarization of the antenna, and the vertical polarization is the cross polarization which is at a very

TABLE 4. Performance comparisons.

Ref.		Range of beam-forming pattern	Beam distribution	Capability of broadside radiation
[9]	LWA	10°~ 60°	unilateral	×
[10]	LWA	15°~ 50°	unilateral	×
[11]	LWA	0°~ 50°	unilateral	√
[12]	LWA	-25°~ -45° & 25°~ 45°	bilateral	×
[16]	microstrip patche array	0°~ 30°	unilateral	√
[17]	patch array	-3°~ 23°	unilateral	√
[18]	microstrip array	-45°~ 45°	bilateral	√
This work	LWA	0°~ 60° (element)	unilateral	√
		-60°~ 60°(array)	bilateral	√

low level. However, keeping the slot boundary symmetrical completely is difficult in fabrication. As the basic fabrication accuracy is about 0.2 mm, so we offset one edge of the slot by 0.2 mm to see the fabrication error. As shown in Fig. 13, a new cross polarization with a significant deviation is observed (the cross polarizations are obtained with respect to the corresponding co-polarization). Therefore, the fabrication errors are actually the main reason of the large discrepancy of cross polarization between the simulation and measurement. The slight increase of the measured result compared with the simulation result is due to the environmental noise.

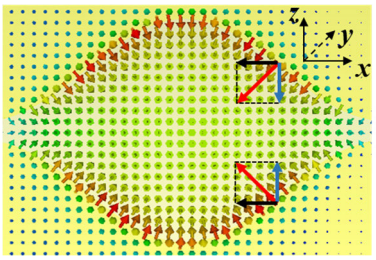

FIGURE 12. Simulated E-field in the radiation aperture at 5.8 GHz.

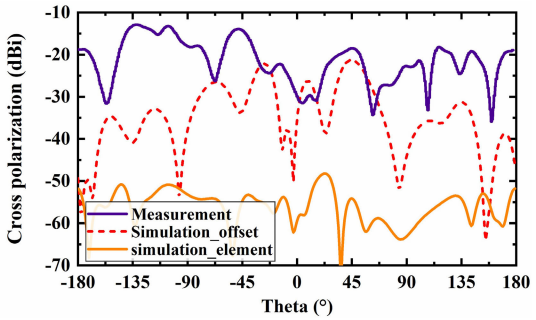

FIGURE 13. Measured and simulated cross polarization of different antenna structures. (The frequency for measurement is 5.9 GHz and the frequencies for simulated curves are 5.8 GHz).

C. BANDWIDTH OF BEAM-FORMING

As the leaky-wave antenna has the capability of frequency scanning, the beam-forming pattern will differ from the anticipative design when the frequency changes. However, as the periodicity of composite slot is not obvious, the influence of frequency changing on radiation pattern is weakened. As can be seen from Fig. 14, the An1 and An2 maintain the secant patterns basically within the range of 5.75 GHz to 5.85 GHz. The change of frequency has a great influence on the initial phase of An2, which further affects the bilateral beam-forming pattern. Thus, the frequency range for the secant pattern of this array is only from 5.78 GHz to 5.82 GHz. As the measured center frequency is changed to 5.9 GHz due to the fabricated errors, the measured radiation patterns near 5.9 GHz are given in Fig. 15, which coincides with the simulation results, showing the property of secant beam-forming.

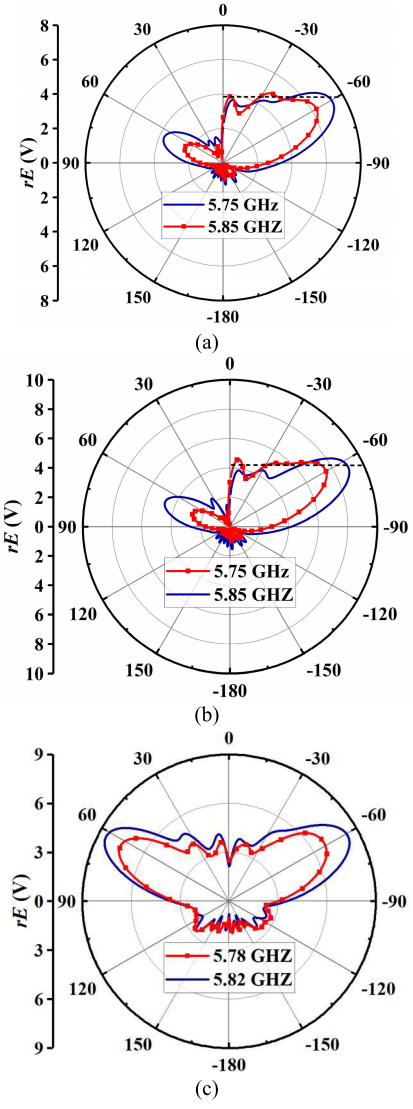

FIGURE 14. Simulated E-patterns of the beam-forming LWAs at different frequencies. (a) An1. (b) An2. (c) Array.

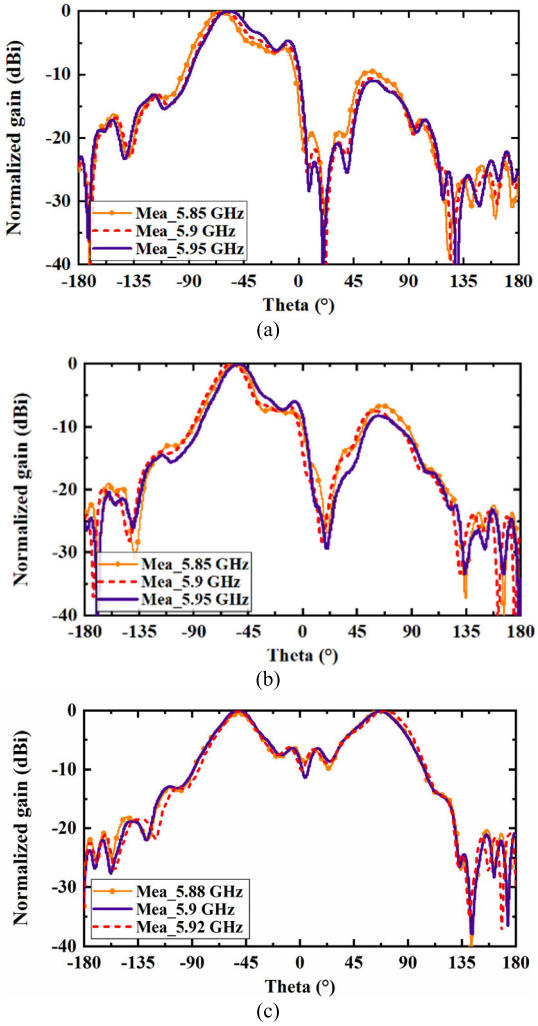

FIGURE 15. Measured radiation patterns of the beam-forming LWAs at different frequencies. (a) An1. (b) An2. (c) Array.

V. CONCLUSION

In this paper, SIW LWAs with secant-distribution patterns are investigated by using the method of superposing radiation from different continuous periodic cosine-shaped slots. The different continuous periodic slots are mapped into one composite slot in a weighted way. The composite slot can naturally remove the OSB, so the beam-forming pattern can cover the broadside direction. The proposed antennas can achieve secant radiation patterns within the range from $-60°$ to $0°$ and from $-60°$ to $60°$ for single LWA element and LWA array, respectively. In addition, the introduction of power recycling network makes the LWA array have the capacity to realize bilateral beam-forming pattern and to improve the radiation efficiency. The antenna with bilateral beamforming pattern proposed in this paper has a wider angular beam-forming range than those of available beamforming antennas, which can cover a longer distance. Therefore, the distance between adjacent base station antennas can be designed longer, reducing the antenna number used in the mobile communication system. The proposed antenna structures are

fabricated and measured, and the measured performances are in good agreement with those of simulations.

REFERENCES

[1] J. Wang, Y. Huang, and D. Li, "Research on the field coverage generated by antennas in confined space," in *Proc. 3rd Asia–Pacific Conf. Antennas Propag.*, Jul. 2014, pp. 775–778, doi: 10.1109/APCAP.2014.6992613.

[2] N. Jaglan, S. D. Gupta, B. K. Kanaujia, and M. S. Sharawi, "10 element sub-6-GHz multi-band double-T based MIMO antenna system for 5G smartphones," *IEEE Access*, vol. 9, pp. 118662–118672, 2021, doi: 10.1109/ACCESS.2021.3107625.

[3] N. Jaglan, S. D. Gupta, and M. S. Sharawi, "18 element massive MIMO/diversity 5G smartphones antenna design for sub-6 GHz LTE bands 42/43 applications," *IEEE Open J. Antennas Propag.*, vol. 2, pp. 533–545, 2021, doi: 10.1109/OJAP.2021.3074290.

[4] V. Thakur, N. Jaglan, and S. D. Gupta, "Side edge printed eight-element compact MIMO antenna array for 5G smartphone applications," *J. Electromagn. Waves Appl.*, vol. 36, no. 12, pp. 1685–1701, Aug. 2022, doi: 10.1080/09205071.2022.2040057.

[5] L. Freytag and B. Jecko, "Cosecant-squared pattern antenna for base station at 40 GHz," in *Proc. IEEE Antennas Propag. Soc. Symp.*, Jun. 2004, pp. 2464–2467, doi: 10.1109/aps.2004.1331872.

[6] J. Liu, D. R. Jackson, and Y. Long, "Modal analysis of dielectric-filled rectangular waveguide with transverse slots," *IEEE Trans. Antennas Propag.*, vol. 59, no. 9, pp. 3194–3203, Sep. 2011, doi: 10.1109/TAP.2011.2161444.

[7] F. L. Whetten and C. A. Balanis, "Meandering long slot leaky-wave waveguide-antennas," *IEEE Trans. Antennas Propag.*, vol. 39, no. 11, pp. 1553–1560, Nov. 1991, doi: 10.1109/8.102768.

[8] Y. J. Cheng, W. Hong, K. Wu, and Y. Fan, "Millimeter-wave substrate integrated waveguide long slot leaky-wave antennas and two-dimensional multibeam applications," *IEEE Trans. Antennas Propag.*, vol. 59, no. 1, pp. 40–47, Jan. 2011, doi: 10.1109/TAP.2010.2090471.

[9] Y. Geng, J. Wang, Y. Li, Z. Li, M. Chen, and Z. Zhang, "New design of beam-formed leaky-wave antenna based on substrate integrated waveguide in a confined space," *IEEE Trans. Antennas Propag.*, vol. 66, no. 11, pp. 6334–6339, Nov. 2018, doi: 10.1109/TAP.2018.2867018.

[10] Y. Geng, J. Wang, Z. Li, Y. Li, M. Chen, and Z. Zhang, "A leaky-wave antenna array with beam-formed radiation pattern for application in a confined space," *IEEE Access*, vol. 7, pp. 86367–86373, 2019, doi: 10.1109/ACCESS.2019.2926212.

[11] Y. Zhang, J. Wang, and Y. Geng, "A beam-formed leaky-wave antenna array with power-recycling feeding network," *Int. J. RF Microw. Comput.-Aided Eng.*, vol. 32, no. 10, Oct. 2022, Art. no. e23295, doi: 10.1002/mmce.23295.

[12] X. Li, J. Wang, Z. Li, Y. Li, Y. Geng, M. Chen, and Z. Zhang, "Leaky-wave antenna array with bilateral beamforming radiation pattern and capability of flexible beam switching," *IEEE Trans. Antennas Propag.*, vol. 70, no. 2, pp. 1535–1540, Feb. 2022, doi: 10.1109/TAP.2021.3111157.

[13] A. A. Oliner and D. R. Jackson, "Leaky-wave antennas," in *Antenna Engineering Handbook*, 4th ed., J. Volakis, Ed. New York, NY, USA: McGraw-Hill, 2007, ch. 11.

[14] F. Xu and K. Wu, "Guided-wave and leakage characteristics of substrate integrated waveguide," *IEEE Trans. Microw. Theory Techn.*, vol. 53, no. 1, pp. 66–73, Jan. 2005, doi: 10.1109/TMTT.2004.839303.

[15] Y. Geng, J. Wang, Y. Li, Z. Li, M. Chen, and Z. Zhang, "Leaky-wave antenna array with a power-recycling feeding network for radiation efficiency improvement," *IEEE Trans. Antennas Propag.*, vol. 65, no. 5, pp. 2689–2694, May 2017, doi: 10.1109/TAP.2017.2681322.

[16] M. V. N. M. Ayyadevara, B. S. N. Kishore, M. VasujaDevi, and E. S. Reddy, "Circularly polarized dual frequency MIMO antenna with cosecant-squared radiation pattern for Ku-band applications," *IEEE Antennas Wireless Propag. Lett.*, vol. 22, no. 6, pp. 1341–1345, Jun. 2023, doi: 10.1109/LAWP.2023.3241958.

[17] H. Yi, L. Li, J. Han, and Y. Shi, "Traveling-wave series-fed patch array antenna using novel reflection-canceling elements for flexible beam," *IEEE Access*, vol. 7, pp. 111466–111476, 2019, doi: 10.1109/ACCESS.2019.2934652.

[18] C. C. Cruz, C. A. Fernandes, S. A. Matos, and J. R. Costa, "Synthesis of shaped-beam radiation patterns at millimeter-waves using transmit arrays," *IEEE Trans. Antennas Propag.*, vol. 66, no. 8, pp. 4017–4024, Aug. 2018, doi: 10.1109/TAP.2018.2836383.

YULU ZHANG was born in Jiangsu, China. She received the B.E. degree from the School of Electronic and Information Engineering, China University of Geosciences (Beijing), Beijing, China, in 2018. She is currently pursuing the Ph.D. degree with the Institute of Lightwave Technology, Beijing Jiaotong University. Her current research interests include the field of beam-forming antennas and arrays.

JUNHONG WANG (Senior Member, IEEE) was born in Jiangsu, China, in 1965. He received the B.S. and M.S. degrees in electrical engineering from the University of Electronic Science and Technology of China, Chengdu, China, in 1988 and 1991, respectively, and the Ph.D. degree in electrical engineering from Southwest Jiaotong University, Chengdu, in 1994. In 1995, he joined as a Faculty Member of the Department of Electrical Engineering, Beijing Jiaotong University, Beijing, China, where he became a Professor, in 1999. From January 1999 to June 2000, he was a Research Associate with the Department of Electric Engineering, City University of Hong Kong, Kowloon Tong, Hong Kong. From July 2002 to July 2003, he was a Research Scientist with Temasek Laboratories, National University of Singapore, Singapore. He is currently with the Key Laboratory of all Optical Network and Advanced Telecommunication Network, Ministry of Education of China, Beijing Jiaotong Univeristy, where he is also with the Institute of Lightwave Technology. His research interests include numerical methods, antennas, scattering, and leaky wave structures.

YUNJIE GENG (Member, IEEE) was born in Hebei, China. She received the B.S. degree in communications engineering and the Ph.D. degree in electrical engineering from Beijing Jiaotong University, Beijing, China, in 2015 and 2020, respectively.

From 2018 to 2019, she was a Visiting Student with the PolyGrames Research Center, Polytechnique Montréal (University of Montreal), QC, Canada. In 2020, she joined as a Faculty Member of the Department of Electrical Engineering, Beijing Jiaotong University, where she is currently an Associate Professor. Her current research interests include beam-forming antennas, beam-steering antennas, and leakywave antennas. She has served as a Reviewer for IEEE TRANSACTIONS ON ANTENNAS AND PROPAGATION, IEEE ANTENNAS AND WIRELESS PROPAGATION LETTERS, IEEE ACCESS, and the *Open Journal of Antennas and Propagation*.